Nuclear Instruments and Methods in Physics Research A 595 (2008) 256–259

Contents lists available at ScienceDirect

Nuclear Instruments and Methods in Physics Research A

journal homepage: www.elsevier.com/locate/nima

Design optimization of the proximity focusing RICH with dual aerogel radiator using a maximum-likelihood analysis of Cherenkov rings

R. Pestotnik [a,*], P. Križan [a,b], S. Korpar [a,c], T. Iijima [d]

[a] Jožef Stefan Institute, Jamova Cesta 39, 1000 Ljubljana, Slovenia
[b] University of Ljubljana, Ljubljana, Slovenia
[c] University of Maribor, Maribor, Slovenia
[d] Nagoya University, Nagoya, Japan

ARTICLE INFO

Available online 8 July 2008

Keywords:
Aerogel radiator
Proximity focusing RICH
Particle identification methods

ABSTRACT

The use of a sequence of aerogel radiators with different refractive indices in a proximity focusing Cherenkov ring imaging detector has been shown to improve the resolution of the Cherenkov angle. In order to obtain further information on the capabilities of such a detector, a maximum-likelihood analysis has been performed on simulated data, with the simulation being appropriate for the upgraded Belle detector. The results show that by using a sequence of two aerogel layers with different refractive indices, the K/π separation efficiency is improved in the kinematic region above 3 GeV/c. In the low momentum region, the focusing configuration (with n_1 and n_2 chosen such that the Cherenkov rings from different aerogel layers at 4 GeV/c overlap) shows a better performance than the defocusing one (where the two Cherenkov rings are well separated).

© 2008 Elsevier B.V. All rights reserved.

1. Introduction

The forthcoming upgrade of the Belle detector at KEK requires an improved particle identification system [1]. The limited available space has led to the decision for a proximity focusing ring imaging Cherenkov detector (RICH) with aerogel as radiator for the forward endcap region. Investigations of the performance of such a detector have given promising results [2]. In particular, the new technique of using two or more aerogel radiators with different refractive indices has improved the resolution of the Cherenkov angle [3]. Essentially, this is achieved by increasing the overall radiator thickness, i.e. photon yield, while avoiding the simultaneous degradation of resolution due to the increase of the emission point uncertainty [4]. Although different combinations of multiple radiators have been experimentally studied, the present analysis is concerned mostly with the case of two radiators. These can be either in a focusing or in a defocusing configuration (Fig. 1). In the former case, the aerogel layer with the higher refractive index is positioned downstream, so that both Cherenkov rings of a single charged particle overlap on the photon detector. On the other hand, in the defocusing configuration the higher refractive index is positioned upstream, so that two well separated rings are obtained for a single charged particle. In both cases an improved overall resolution of the particle velocity is obtained.

We studied the K/π separation efficiency for different aerogel configurations by varying several detector parameters. Our results are based on the data from a GEANT4 simulation [5] of the simple proximity focusing RICH with aerogel as radiator. The detector hits are used to evaluate the likelihood function for different particle hypotheses. The separation efficiencies for different aerogel configurations are presented in Section 4.

2. Simulated data

The charged particle transport and generation of Cherenkov photons in the aerogel layers, Rayleigh scattering in aerogel (with 40 mm transmission length at $\lambda = 400$ nm) and propagation of the photons to the photosensitive plane were simulated using the simulation toolkit Geant4 [5]. The simulated detector is similar to the apparatus used in test measurements [3]. It consists of layers of aerogel layers with a fixed distance (20 cm) between the entrance surface of the radiators and the front surface of the photon detector. The photons are detected with Hamamatsu H8500 PMTs, which have a 2 mm thick quartz window (Fig. 1).

The data have been simulated for a single charged particle traversing perpendicularly the Cherenkov ring imaging detector. In simulation we assumed a photon detector consisting of 6.1 × 6.1 mm pads [3] with positionally uniform response of the bialkali

* Corresponding author. Tel.: +386 1 477 3900; fax: +386 1 425 7074.
E-mail address: rok.pestotnik@ijs.si (R. Pestotnik).

0168-9002/$ - see front matter © 2008 Elsevier B.V. All rights reserved.
doi:10.1016/j.nima.2008.07.019

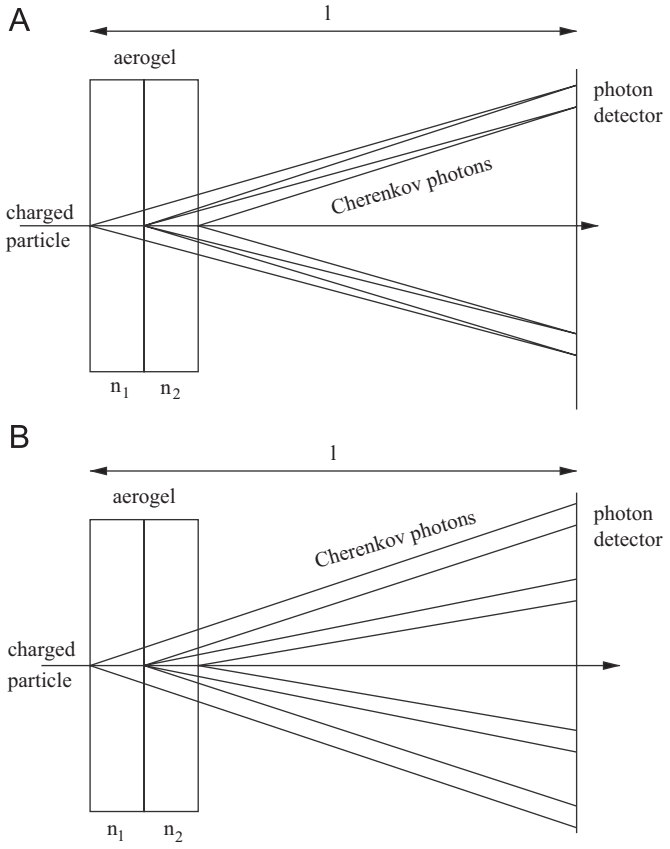

Fig. 1. Simulated counters: in the focusing configuration with refractive indices of the 15 mm thick layers $n_1 = 1.043$ and $n_2 = 1.05$ (A), the Cherenkov rings emitted from different radiators overlap on the photon detector. In the defocusing configuration with refractive indices of the 15 mm thick layers $n_1 = 1.05$ and $n_2 = 1.03$ (B), the Cherenkov rings from different aerogel layers are well separated. The counters were compared to the configuration where a single radiator layer of $n = 1.05$ with the same total thickness of 30 mm was used.

photocathode [6]. We adjusted the photodetection efficiency in such a way that the resulting number of detected photons per ring agrees with the measured average number of detected photons ($N_{\text{p.e.}} = 6$) for 2 cm aerogel with refractive index 1.05 [2]. To account for other contributions to the resolution, the emission direction of Cherenkov photons is smeared by 8 mrad [2,7]. In such a way the resulting simulated resolution ($\sigma_\theta = 14$ mrad) also agrees with the measurements. We also neglected any cross-talk between neighboring pads and we assumed binary electronics, i.e. no distinction was made between cases when a channel is hit by one or by multiple photons.

Single tracks are simulated for kaons and pions with momenta up to 5 GeV/c, which is above the kinematic limit of the decay products in the Belle spectrometer [1].

In addition to the Cherenkov photons from charged particles, background hits are simulated uniformly over the detection surface with a density of up to 125 hits/m^2. This is a factor of 4 higher than what is expected during the operation of the detector.

3. Likelihood function

The construction of a likelihood function follows Baillon [8] and Forty [9]. With a given hypothesis h for the charged particle mass (either pion or kaon) and for given track geometry, a likelihood function is constructed for each track. This consists of the product of probabilities p_i of individual pixels i being hit:

$$L = \prod_{\text{all pixels}} p_i. \tag{1}$$

The probability of pixel i recording m_i hits is Poissonian:

$$p_i = \frac{e^{-n_i} n_i^{m_i}}{m_i!} \tag{2}$$

where n_i is the expected, i.e. calculated average number of hits on the particular pixel. Obviously, n_i will depend on the hypothesis h for the particle type. Probabilities for a pad to be hit ($m_i > 0$) or not ($m_i = 0$) are

$$p_i = \begin{cases} e^{-n_i} & \text{for } m_i = 0 \\ 1 - e^{-n_i} & \text{for } m_i > 0. \end{cases} \tag{3}$$

We take the logarithm of the product of likelihoods, separate contributions of hit and non-hit pixels and constrain the number of expected hits N for a given hypothesis to the sum of expected average number of hits on the detector [9] to obtain

$$\ln L = -N + \sum_{\text{hit } i} \ln(e^{n_i} - 1). \tag{4}$$

The obvious advantage of this procedure is that one now has to calculate the average number of hits, i.e. the hit probabilities n_i only for the hit pixels.

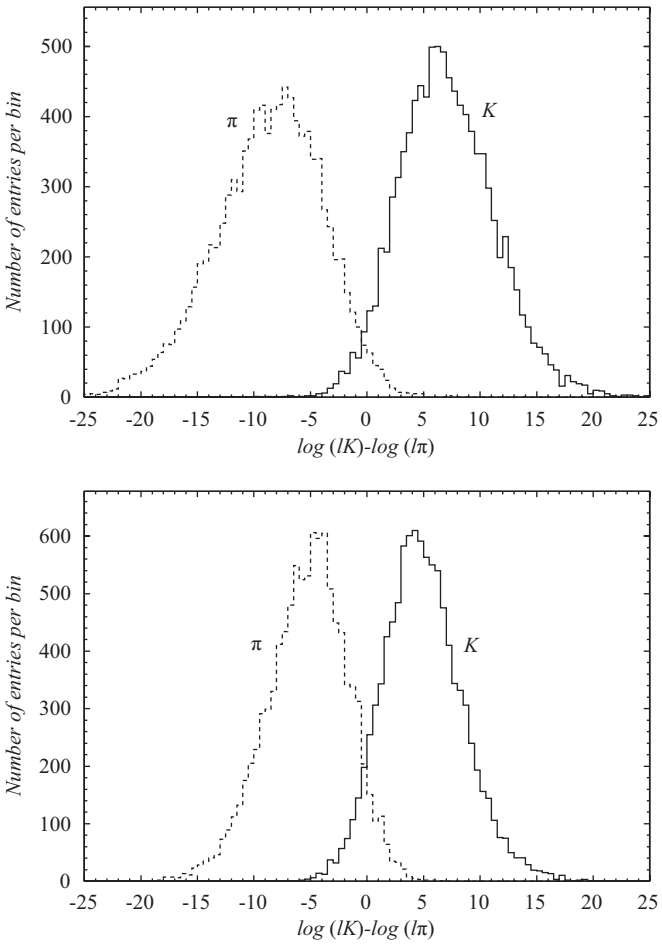

Fig. 2. The log likelihood difference of the kaon and pion hypotheses for pions (dashed line) and kaons (full line) at 4 GeV/c for the focusing dual radiator (top) and a single radiator configuration (bottom).

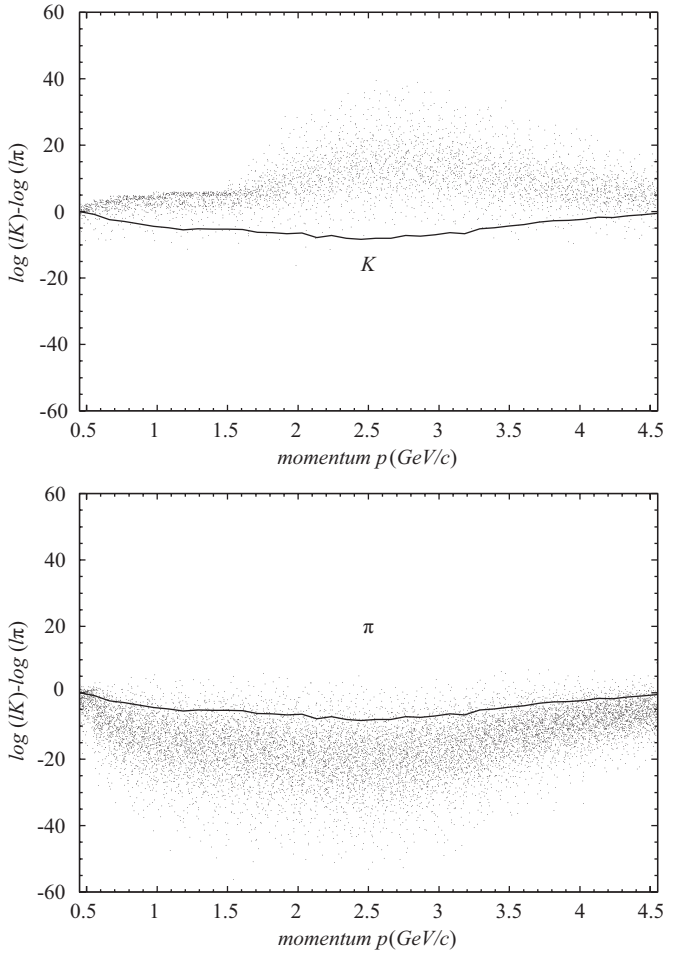

Fig. 3. Momentum dependence of the log likelihood difference of the kaon and pion hypotheses for kaons (top) and pions (bottom) for the focusing configuration. The solid line represents a cut for which ≈ 1% of the pion events would be misidentified as kaons.

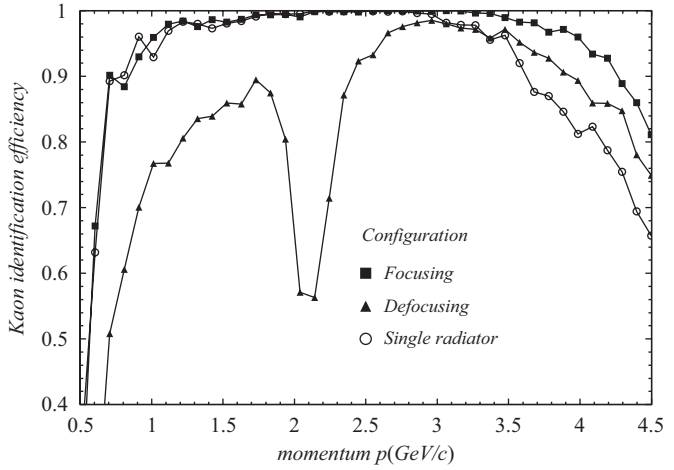

Fig. 4. The kaon identification efficiency as a function of momentum for different configurations: the focusing (squares), the defocusing (triangles) and the single radiator configuration (open circles) for 1% pion misidentification probability.

4. Results

We first illustrate the improvement in the K/π separation obtained with the dual radiator in the focusing configuration (Fig. 2). The number of particles is plotted as a function of the difference of the logarithms of the likelihoods for the kaon and pion hypotheses. By comparing the focusing configuration to the single radiator configuration, the advantage of the focusing configuration becomes obvious. For 1% probability to misidentify a pion, 96% of the kaons are correctly identified in the focusing configuration compared to 87% in the homogeneous radiator case.

The difference in the logarithm of the likelihood as a function of particle momentum is shown for the focusing configuration in Fig. 3. For particles known to be pions, the distribution seems to be well separated from those known to be kaons. Fig. 4 shows the efficiency for kaons to be properly identified for 1% probability to misidentify a pion for different configurations: the focusing and the defocusing dual radiator configuration and the single radiator configuration. Note the dip in the kaon identification efficiency of the defocusing configuration slightly above 2 GeV/c, which can be attributed to the overlap of pion rings from one radiator with the kaon rings from the other radiator (Fig. 5).

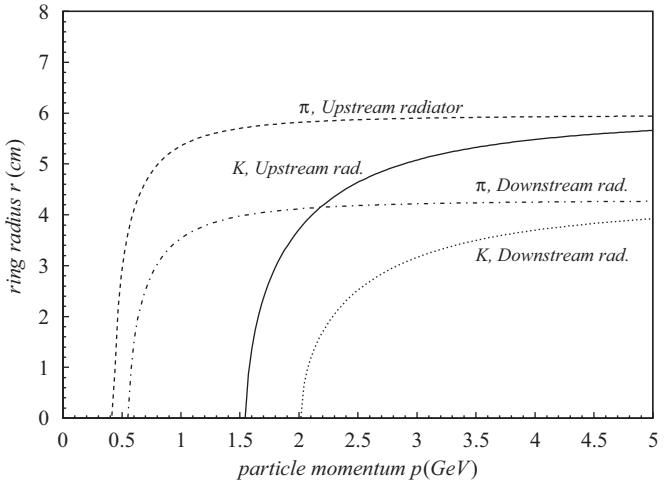

Fig. 5. The variation of ring radii with momentum for pions and kaons for the defocusing configuration. Note the overlapping of Cherenkov rings from different radiator layers above 2 GeV/c.

It can also be seen that both focusing and defocusing configurations are significantly better than the single aerogel configuration in the region above 3 GeV/c. For the low momentum region, however, the focusing configuration as well as the homogeneous radiator perform better than the defocusing configuration. The reason can be attributed to the fact that Cherenkov threshold for kaons is at 2.0 GeV for one of the layers in the defocusing radiator ($n = 1.03$), thus leading to only approximately half of the photons being detected below 2.0 GeV. Since the Cherenkov rings are separated, it is also more sensitive to the random background.

5. Conclusions

To study the particle identification performance of various configurations of the proposed proximity focusing RICH with aerogel as the radiator, we have constructed and evaluated the likelihood function for different particle hypotheses. The results show that by using a sequence of two aerogel layers with different refractive indices, the K/π separation efficiency is increased in the kinematic region above 3 GeV/c. A dual layer configuration seems to perform better than the defocusing one, which has a dip in the efficiency, where the rings for pion and kaon hypothesis from different radiator layers overlap.

Acknowledgments

This work was supported in part by the Slovenian Research Agency under Grant nos. J1-6559 and J1-9840.

References

[1] K. Abe, et al., Letter of intent for KEK super B factory, KEK Report 2004-4, 2004.
[2] T. Matsumoto, Nucl. Instr. and Meth. A 521 (2004) 367.
[3] T. Iijima, et al., Nucl. Instr. and Meth. A 548 (2005) 383.
[4] P. Križan, et al., Nucl. Instr. and Meth. A 565 (2006) 457.
[5] S. Agostinelli, et al., Nucl. Instr. and Meth. A 506 (2003) 250.
[6] Hamamatsu R5900 PMT data sheet.
[7] P. Križan, et al., Nucl. Instr. and Meth. A 553 (2005) 58.
[8] P. Baillon, Nucl. Instr. and Meth. A 238 (1985) 341.
[9] R. Forty, Nucl. Instr. and Meth. A 433 (1999) 257.